Ecol Res (2017) 32: 117–128
DOI 10.1007/s11284-016-1423-2

ORIGINAL ARTICLE

Yuuki Tsunoda · Shoko Furukawa · Hiromi Mizunaga

How does the longevity of *Sasa kurilensis* ramets respond to a light gradient? An analysis of ontogenetic changes to hydraulic resistance and carbon budget within a ramet

Received: 24 April 2016 / Accepted: 5 December 2016 / Published online: 21 December 2016

Abstract We investigated how *Sasa kurilensis* ramet longevity differs under three light conditions. Ramet longevity is an important factor affecting the abundance of ramet populations and their biomass. The objectives of this study were to clarify: (1) whether ramet longevity varies spatially along a gradient of light conditions; (2) whether physiological functions, including water transport in culms, change with ontogenesis; (3) whether ramet longevity is associated with the most effective turnover for gaining a carbon profit within a ramet following a cost-benefit model or is affected by other factors such as death caused by a decline in physiological function. We analyzed *S. kurilensis* ramet longevity, hydraulic resistance, photosynthetic rate, and carbon content. We then estimated the ramet carbon budget. The longevity of *S. kurilensis* ramets was 2.8–4.5 years in Beneath-patch plots, 5.8–8.7 years in Edge-patch plots, and 1.6–2.2 years in Open-patch plots. Although leaf photosynthetic activity was stable, the instantaneous photosynthetic rate decreased during clear days in the open area. This may have been due to increased ramet hydraulic resistance. The rotation period of the most efficient carbon budget quantified by ecophysiological measurements was consistent with ramet longevity in Open-patch (2 years) and Edge-patch (5 years) sites. Meanwhile, the longevity of ramets grown under canopies was inconsistent with the cost-benefit model rules for a carbon budget because the carbon gain was low throughout the ramet life span.

Y. Tsunoda
The United Graduate School of Agricultural Science, Gifu University, 1-1 Yanagito, Gifu, Gifu 501-1193, Japan

S. Furukawa · H. Mizunaga (✉)
Faculty of Agriculture, Shizuoka University, 836 Ooya, Suruga-ku, Shizuoka, Shizuoka 422-8017, Japan
E-mail: mizunaga.hiromi@shizuoka.ac.jp
Tel.: +81-54-238-4841

Present address: S. Furukawa
16 Kurikoma Hishinuma Shoubu, Kurihara, Miyagi 989-5323, Japan

Keywords Cost-benefit model · Dwarf bamboo · Life span · Ramet age · Water stress

Introduction

Sasa kurilensis (Rapr.) Makino and Shibata, an evergreen clonal dwarf bamboo, is a dominant species covering beech (*Fagus crenata*) forest floors in the snowy regions of Japan. Its thick vegetation strongly competes with tree seedlings (Nakashizuka and Numata 1982; Nakashizuka 1987, 1988). This dwarf bamboo can grow under a broad understory light gradient and in open sites (Wijestinghe and Hutcings 1997; Lei and Koike 1998). Saitoh et al. (2000) suggested that photosynthetic products in the gaps of dwarf bamboo leaves are transported to the shaded ramets in the understory through rhizomes based on the observation that gap distances affected plant biomass more than light conditions. They also suggested this ability to grow in shaded conditions is the result of shade tolerance and physiological integration among ramets established in gaps and the understory (Saitoh et al. 2002, 2006; Saitoh and Seiwa 2007).

Ramet longevity serves as an important component of ramet population dynamics and affects the biomass of a community. A few previous studies reported that ramet longevity is 1 year for *Sasa nipponica* (Terai et al. 2009), 2.8–3.6 years for *Sasa veitchii*, *Pleioblastus akebono*, and *Pseudosasa awatarii* f. *nana* (Shibata 1992), and 6.3–9.6 years for *S. kurilensis* (Yajima et al. 1997). However, these studies did not address the influence of light availability on ramet longevity.

Plausible mechanism that ramet longevity varies with growing light conditions may be explained by the cost-benefit of the carbon budget within a ramet unit. Chabot and Hicks (1982) reviewed the factors that determine leaf longevity in various environments, and concluded that leaf longevity is regulated by the balance between

the benefits of net carbon gain created by keeping a leaf and the cost of replacing leaves in terms of carbon or nutrients. Kikuzawa (1991) developed a simple model for estimating the cost-benefit of the carbon budget for a single leaf. This model assumes that optimal leaf longevity is achieved when the carbon profits over the life span of a leaf are maximized. This is based on three factors, namely initial photosynthetic ability, initial leaf formation costs, and decreasing rates of photosynthetic output over time. The relationships between leaf longevity and these factors were determined based on the following observations. Leaf longevity is shorter in well-lit habitats than in dark habitats for *Castanopsis sieboldii*, *Quercus acuta*, *Camellia japonica*, *Cleyera japonica*, *Cinnamomum japonicum*, *Illicium anisatum*, and *Maesa japonica* (Hikosaka 2005). Several studies reported that species with a longer leaf life span have a lower photosynthetic capacity per unit mass and unit area, a lower nitrogen concentration per unit mass, and a higher leaf mass per area irrespective of life form, phylogeny, and biomes (Reich et al. 1997, 1999; Wright et al. 2004). Leaf longevity is positively correlated with the leaf construction cost (Williams et al. 1989). A decrease in the photosynthetic rate with aging also affects leaf longevity (Matsumoto 1984a, b; Kikuzawa 1988, 1989, 1991).

The theoretical model for a cost-benefit relationship of a carbon budget is likely applicable to the analysis of ramet longevity, although the carbon budget of a ramet is more complex than that of a single leaf. A bamboo ramet consists of multiple leaves and a culm, and regenerates new branches with leaves throughout the life span of a ramet. The formation of *S. kurilensis* ramets requires an investment in carbon not only during the initial year but also in subsequent years. The photosynthetic ability of a ramet can be related to the photosynthetic potential of leaves in the absence of water stress, total leaf area, and the effects of water stress. Water stress due to increases in stem hydraulic resistance (Ryan and Yoder 1997) induces stomatal closure, which decreases the photosynthetic rate (Holbrook and Lund 1995). In *S. kurilensis* ramets, tylose formation was observed in xylem vessels of a 4-year-old culm (Kawase et al. 1984). If the number of tylose-filled vessels increase ontogenetically, culm hydraulic resistance may also increase ontogenetically.

Although the relationship between the carbon budget in a ramet unit and ramet longevity is complex, determining whether increasing longevity maximizes the efficiency of the carbon budget may help characterize the contribution of a ramet to the genet under specific light conditions. A specific longevity that maximizes carbon budget efficiency may positively influence the contribution of a ramet to genet productivity, even if the ramet does not have an autonomous carbon economy. If a ramet has a function other than sequestering carbon, longevity does not need to be prioritized to maximize carbon production.

In this study, we tested the hypothesis that variations in ramet longevity under different light conditions are explained by optimal ramet turnover predicted using a theoretical model for cost-benefit relationships of a carbon budget. We measured the maximum gross photosynthetic rate (*Pmax*), dark respiration (*Rd*), ramet longevity, hydraulic conductance of a ramet, and leaf and stem dry masses. Our objective was to clarify the following points: (1) whether ramet longevity varies spatially along a gradient of light conditions; (2) whether the longevity of a ramet corresponds to the most effective turnover model for gaining carbon profits within a ramet. Because the most effective turnover model is based on three factors (i.e., initial photosynthetic ability, initial cost of tissue formation, and decreasing rates of photosynthetic output over time), we determined the carbon gains and costs for different ramet age classes. Additionally, we investigated decreases in physiological functions during ontogenesis, including changes in water transport in culms, leaf photosynthetic capacity, and total leaf area per ramet. We used a theoretical model for the cost-benefit relationship of a carbon budget that considered leaf longevity. We also examined whether longevity is affected by other factors such as wilting caused by water stress.

Methods

Study site

The study sites were located at 900 m above sea level on the southeastern slopes of Mt. Naeba, Japan (36°55′N, 138°46′E). The study plots were established at two adjacent locations. The first site was in a 70-year-old second-growth *Fagus crenata* forest, while the second location was in a gap within a 50-m^2 area adjacent to a second-growth stand. The mean annual precipitation at the nearest weather station located 2.9 km southwest of the study site was 2230 mm based on records from 1988 to 2010 (Japanese Bureau of Meteorology website; http://www.data.jma.go.jp/obd/stats/etrn/). A large proportion of the precipitation was in the form of snow during winter (i.e., 3–4 m accumulation). The mean air temperature at the study sites was 8.5 °C in 2011. Snow remained on the ground until mid-May, and beech leaves began to flush in late April or early May. Leaves started to change color in autumn in late October. The *S. kurilensis* current-year leaves flushed in late July, and the leaf area peaked in August. *Fagus crenata* trees dominated the upper-canopy layer in the study areas, while other species, including *Quercus mongolica*, occurred sporadically. The bedrock in the study sites was predominantly andesite and basalt, and was covered with a moderately moist brown forest soil.

Ramet longevity in *Sasa kurilensis* vegetation

We established 50, 58, and 50 1-m^2 plots in a *S. kurilensis* patch beneath a beech forest habitat (i.e., Beneath-patch), as well as 50, 80, and 50 plots in an open area (i.e., Open-patch) in 2011, 2012, and 2013, respec-

tively. Additionally, 100 and 50 plots were established at the edge of a beech forest habitat (i.e., Edge-patch) in 2012 and 2013, respectively. We recorded ramet age based on the divergence pattern of branching (Oshima 1961) and diameter at the base of culms in all plots. We defined a ramet as a unit consisting of a culm, leaves, and the branches attached to the culm without rhizomes or roots. Thus, an age census was conducted for all ramets in 158, 150, and 180 Beneath-, Edge-, and Open-patch plots, respectively.

We also calculated the mean ramet longevity for each plot as the ratio of the total number of ramets to the number of current-year ramets as previously described (Yajima et al. 1997). This method was used because the complex divergence of culms may occasionally lead to errors in age estimations.

Ramet hydraulic resistance

We classified ramets into specific age classes (i.e., 0, 1, 2, 3, 4, and >5 years), and sampled one or two ramets with culms having diameters of 8.5–9.5 mm for each age class in all patches. We installed handmade sap-flow sensors according to the stem heat balance method, which calculates heat loss due to sap flow within the stem to culms 50 cm above the ground surface (Sakuratani 1981). The sensors were covered by heat insulators to prevent heat advection, and by plastic sheets to provide protection from rain.

We calibrated the sap flow measurements of the stem heat balance method as a true value based on the culm water flow generated by added pressure. We placed a cut end of a culm section into a water pool installed inside a 3000F01 pressure chamber (Soil Moisture Equipment Corp., Santa Barbara, CA, USA), while the other cut end was connected to a plastic tube with a measuring pipette. We attached the sap-flow sensor to the culm section, and generated sap flow through the sample culm at a positive pressure induced by the pressure chamber. Five chamber pressure levels were used to obtain a wide range of sap flow velocities. We logged electric voltages from three pairs of thermocouples in a sensor and calculated the sap flow rate according to the method described by Sakuratani (1981). We also read the scale of the measuring pipette during a given period. The measuring period increased (i.e., 30 s, and 1, 2, 5, and 10 min) with decreasing chamber pressure to avoid errors at low sap flow velocities. We generated a regression line between the sap flow rate calculated using electric voltages from the sap-flow sensor and the volumetric flow rate for calibrations. We regressed the slope of the calibration line with culm diameter for use with field measurements.

We recorded meteorological data [e.g., photosynthetic photon flux density (PPFD), air temperature, and humidity] for the top of the dwarf bamboo trees using G1118 photodiodes (Hamamatsu Photonix, Hamamatsu, Japan) that were previously calibrated with a Li-190R quantum sensor (LiCor, Inc., Lincoln, NE, USA), thermocouple, and RSH-1010 moisture sensor (Espec Mic Corp., Oguchi, Japan). Measurements were taken every minute and logged for 30 min on average during the growing season from May to November, which corresponded to the snow-free season. The sap-flow and micro-climate data were recorded every 30 s with a GL820-UM-80 data logger (Graftec Corp., Kanagawa, Japan) in the Open-patch plots on August 10–14, 2011, and in Beneath-patch plots on September 8–17, 2011. Although the Open- and Beneath-patch plots were analyzed at different times, the climatic conditions at all plots were similar in August and September (Fig. 1).

We measured xylem pressure potentials of one to three leaves from each sample ramet before dawn and during the day (i.e., 11:00–13:00) in the Open- and Beneath-patch plots on a clear day during the period in which the sap-flow rate was measured. We calculated the average sap-flow rate for the period 20 min before to 20 min after the potential measurement because it took 40 min to measure the xylem pressure potentials of all leaves. Therefore, measurements were made at 40-min intervals for each ramet. The average sap-flow rate

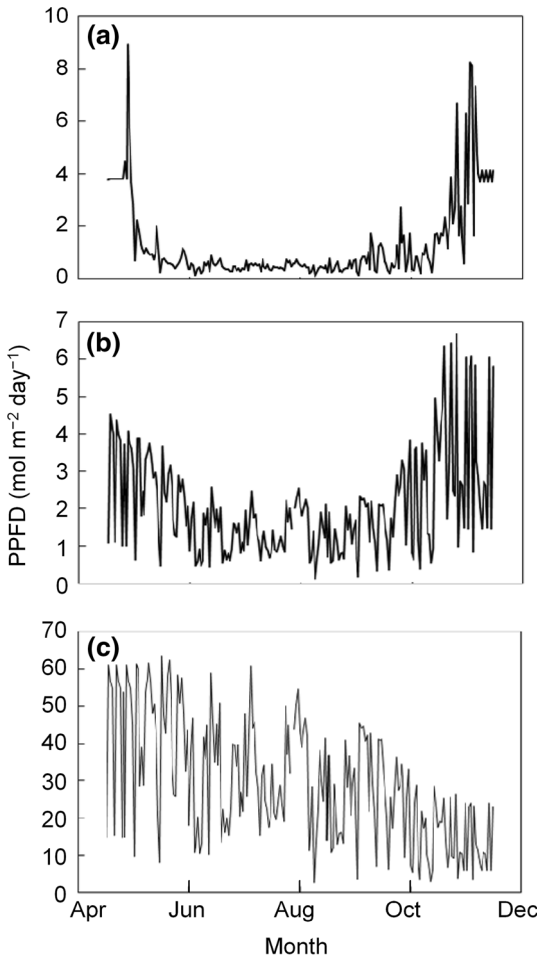

Fig. 1 Monthly changes in photosynthetic photon flux density (PPFD) above *Sasa kurilensis* patches in 2013. **a** Beneath-patch, **b** Edge-patch, and **c** Open-patch

changed by less than 7% during the 40-min period. We calculated hydraulic resistance through culms using Eq. 1:

$$Rh = \frac{\left(\psi_{predawn} - \psi_{day}\right) \cdot CA}{SF_{40}}, \quad (1)$$

where Rh, $\Psi_{predawn}$, Ψ_{day}, CA, and SF_{40} represent hydraulic resistance in a ramet per culm cross-section area (MPa s mol^{-1} m^2), predawn xylem potential (MPa), xylem potential during the day (MPa), culm section area (m^2), and sap-flow rate at 40-min intervals (mol s^{-1}), respectively.

Photosynthetic measurements

Prior to the current study, a photosynthetic-light response curve was prepared using an LI-6400 portable photosynthesis system (LiCor, Inc.) once per month from June to November in 2005. Analyses were conducted in an *S. kurilensis* community of a beech forest located at 1500 m above sea level on the eastern slope of Mt. Naeba, at sites 5 km from the patches in the current study. These analyses were conducted to clarify the pattern of seasonal changes and the differences in photosynthetic rates among leaf ages. The photosynthetic rate was measured under the following conditions: PPFD: 0, 50, 100, 200, 350, 500, 700, 1000, and 1500 μmol m^{-2} s^{-1}; CO_2 concentration: 350 ppm; relative humidity: 60–75%. The measuring temperature (i.e., 15–22 °C) was the mean monthly temperature including the measuring day (Appendix Table 2). We analyzed three current-year leaves and three 1-year-old leaves from each ramet grown in an open area or beneath a canopy. Samples were sufficiently watered prior to measurements to avoid the effects of drought stress. Based on the preliminary experiment, the *Pmax* was almost constant from May to October, but the values in November were 74.3% of that in the other seasons (Appendix Table 3). The *Pmax* value of 1-year-old leaves was 75.1% of that of current-year leaves throughout the growing season, which suggested leaf age affected photosynthetic activities. Additionally, the maximum *S. kurilensis* leaf longevity is 2 years. The *Rd* value for all months (except August) was 63.1% of that of August. The *Rd* of 1-year-old leaves was 61% of that of current-year leaves throughout the growing season (Appendix Table 3).

We recorded the diurnal changes to photosynthetic activities of five current-year leaves in ramets of each age class and in each plot using a portable ADC photosynthesis system (Analytical Development Co., Hoddesdon, England) to observe the mid-day-depression of photosynthetic activities. Measurements were taken at 1-h intervals from 5:00–6:00 to 18:00–19:00 on 6 clear days, with adjustments made based on the instantaneous ambient temperatures (Table 1). The photosynthetic rate was measured for leaves at the top of ramets, which is where most *S. kurilensis* leaves were distributed.

We measured *Pmax* and *Rd* values for five intact leaves for each age class and patch in mid-August 2012 using the LI-6400 portable photosynthesis system under the following conditions: CO_2 concentration in ambient air: 360 ppm; leaf temperature: 25 °C; PPFD: 1200 μmol m^{-2} s^{-1}. Analyses were conducted at night after watering samples for 30 min to prevent leaf water deficits.

Estimation of mid-day-depression of photosynthetic activities

The photosynthetic-light response curve was approximated using Eq. 2 (Thornley et al. 1976):

$$P(I) = \frac{\varphi I + Pmax - \left\{(\varphi I + Pmax)^2 - 4\varphi I\theta Pmax\right\}^{0.5}}{2\theta} - Rd, \quad (2)$$

where $P(I)$ is the photosynthetic rate when PPFD is I, φ is the initial slope calculated from the photosynthetic rate at a PPFD < 50 μmol m^{-2}, θ is the convexity of the curve obtained from the preliminary experiment, and *Pmax* and *Rd* are the maximum gross photosynthetic and dark respiration rates for each patch, respectively.

We considered the difference between the observed photosynthetic rate (i.e., diurnal change values determined using the ADC photosynthesis system) and the estimated rate (i.e., with PPFD levels during measurements used in the equation) to represent the mid-day-depression caused by water stress. These measurements

Table 1 Measurement dates for diurnal changes in photosynthetic rate, light conditions, and average daily total photosynthesis

Patch	Measurements date	PPFDt (mol m^{-2} day^{-1})	PPFDm (mol m^{-2} day^{-1})	Average daily total photosynthesis (mmol m^{-2} day^{-1})					
				0 year	1 year	2 years	3 years	4 years	5 years
Beneath	Sep. 7, 2012 5:00—19:00	37.65	0.81	21.66	22.87	24.16	19.89	21.65	19.53
Edge	Sep. 2, 2012 5:00—18:00	36.68	1.33	49.37	43.54	46.70	44.83	42.12	42.31
Open	Sep. 5, 2012 5:00—19:00	41.12	32.74	317.25	269.26	261.72	235.79	220.74	218.74
	Aug. 13, 2013 5:00—19:00	50.42	37.84	330.11	332.47	263.35	221.73	173.95	202.41
	Sep. 18, 2013 6:00—18:00	43.97	33.27	344.59	300.53	226.85	232.31	196.84	191.38
	Oct. 14, 2013 6:00—18:00	32.84	23.44	288.50	259.64	274.69	220.92	229.49	241.20

PPFDt daily total photosynthetic photon flux density (PPFD) at the observation tower, *PPFDm* daily total PPFD in the field plot

were taken after ensuring the maximum values recorded by the ADC and LI-6400 units were nearly equal to each other. This was done because the mid-day photosynthetic rate may be lower than that indicated by the light response curve (i.e., mid-day-depression) (Holbrook and Lund 1995; Bassow and Bazzaz 1998). The mid-day-depression rate (*DEP*) was defined as the proportion of the decrease in the value of the photosynthetic-light response curve at a given PPFD.

Ramet carbon content

We sampled 10 ramets (age class: 0–5) in each patch in October 2012 to determine the biomass of leaves, branches, and stems. We measured leaf area using the GTS600 image scanner (Seiko Epson, Nagano, Japan). The leaves and culms were then dried at 80 °C for 3 days to determine dry weights. The allometric relationships among culm, branch, and leaf weights were established for each age class and patch. We also sampled three leaves per ramet and three 15–25-cm-long culm sections harvested at the base, center, and tip for carbon content analyses using an NC analyzer (Sumigraph NC-95A SCAS, Osaka, Japan). The carbon mass of each ramet organ was estimated by multiplying the mean carbon content and biomass values for each organ.

Statistical analysis

We conducted multiple comparisons using the Kruskal–Wallis method to examine the differences in ramet longevity among patches. Generalized linear models (GLMs) were established for two response variables, namely hydraulic resistance (*Rh*) in culms and instantaneous photosynthetic rate (*Pn*) for each observation date. Explanatory variables included combinations of ramet age (*AGE*) and patch (*PATCH*) for *Rh* in culms, and *AGE*, *PPFD*, and vapor pressure deficit (*VPD*) for *Pn* data. Appendix Table 4 provides details regarding the best GLM for hydraulic resistance. We selected the best models using the minimum Akaike's Information Criterion (AIC) value for each response variable.

We also established two *DEP* estimation models using generalized linear mixed models if mid-day-depression of the photosynthetic rate was observed. The random effect in both models was measuring date (*DATE*), while the interaction between *AGE* and *VPD* in Model 3-1 and only *VPD* in Model 3-2 were the fixed effects. The logit link function was used for the models. The *Pmax* and *Rd* values for the current-year leaves were analyzed by one-way analysis of variance to verify differences among ramet age classes. All statistical analyses were completed using R-statistical software (R 3.2.0). Model numbers and details are provided in Appendix Tables 3, 4, 5.

Estimation of ramet carbon budget

An ontogenetic carbon budget was calculated using a model ramet as follows. The model ramet weight was assumed to be the same as the mean weight of the sampled current-year culms in each patch, and was considered to be constant after 7 years. The model ramet leaf and branch biomasses were estimated from allometric relationships in each age class. Thus, the ramet leaf and branch biomasses changed over 8 years, while the culm biomass remained constant.

We estimated the net photosynthetic rate under well-watered conditions using Eq. 2, substituting measured *Pmax*, *Rd*, and instantaneous PPFD values at the top measurement plot for each patch and age class. We assumed all ramet leaves received the same PPFD as the top of the vegetation, and ignored the vertical light extinction because most leaves were positioned horizontally at the ramet tops. Multiplying the photosynthetic rate measured under well-watered conditions by *DEP* obtained using either Model 3-1 or Model 3-2 provided the instantaneous net photosynthetic rate while accounting for stomatal closure. We summed the product of the instantaneous net photosynthetic rate and leaf area per ramet during the growing season from May to November to obtain the annual carbon gain by ramet leaves. In this procedure, we assumed the leaf *Pmax* and *Rd* values exhibited the same seasonal and ontogenetic changes as the preliminary measurements. The *Pmax* value was assumed to be constant from May to October, but was 75% of the *Pmax* value in November. We also assumed the leaf *Rd* values for all months (except August) were 63% of the *Rd* value in August. The *Pmax* and *Rd* values of 1-year-old leaves were assumed to be 75.1 and 61% of the corresponding values for current-year-old leaves, respectively.

We estimated the respiration of non-assimilating organs based on the Arrhenius equation for *Sasa senanensis* culm respiration and temperature described by Nishimura et al. (2004). We summed the respiration values during the seasons and added the annual carbon gain in leaves to obtain the annual carbon gain per ramet.

We determined the carbon investment, including construction costs for leaves and non-assimilating organs such as culms and branches, based on carbon content and newly produced biomass. We calculated the annual carbon profit as the difference between annual carbon gain and carbon investment. Dividing the cumulative carbon profit from year 0 to specific years according to ramet age provided the mean carbon profit rate during each part of the ramet lifespan, which Kikuzawa (1991) referred to as the "marginal gain."

Results

The mean daily PPFD in the Edge- and Beneath-patch plots was highest during the leafless season (i.e., May

and November). During the beech tree growing season, the mean daily PPFD was 20 and 80 times higher in the Open-patch plots than in the Edge- and Beneath-patch plots, respectively (Fig. 1).

Ramet density decreased with age. Six-year-old ramets had one-fifth of the current-year-old ramet density in the Beneath-patch plots. In contrast, the ramet density in the Edge-patch plots remained relatively stable for up to 7 years. the Open-patch plot ramet density was 5–10-fold higher than that of the other two plots, particularly for the current-year-old ramets. However, the density of 1-year-old ramets in the Open-patch plots was almost half of that of current-year-old ramets in the same plots (Fig. 2). A significant difference in ramet age distribution was detected between all patch pair combinations ($P < 0.001$) according to Kruskal–Wallis tests. The mean longevities calculated by dividing the total number of ramets by the number of current-year-old ramets were 2.8 (2011), 4.5 (2012), and 4.4 (2013) in Beneath-patch plots, 5.8 (2012) and 8.7 (2013) in Edge-patch plots, and 2.2 (2011), 1.6 (2012), and 2.1 (2013) in Open-patch plots.

Ramet hydraulic resistance increased with ramet age ($P = 0.003$). Five-year-old ramets had twice the hydraulic resistance of current-year-old ramets (Fig. 3). Model 1-1, which included *AGE* and *PATCH*, was selected as the best model for culm hydraulic resistance, and both factors significantly affected hydraulic resistance. Appendix Table 5 provides details for the best GLMs for instantaneous photosynthetic activities on each measuring date.

The *Pmax* and *Rd* values did not exhibit significant differences among age classes (one-way analysis of variance; $P > 0.05$) in all patches (Fig. 4). The *Pmax* value was 3.79–5.59 μmol m^{-2} s^{-1} in the Beneath- and Edge-patch plots, while it was 11.64–13.50 μmol m^{-2} s^{-1} in the Open-patch plots. The absolute *Rd* values were more negative in the Edge-patch plots than in the other patches.

For diurnal changes, the maximum values of instantaneous photosynthetic rates were 3–5-times higher in the Open-patch plots than in the Edge- and Beneath-patches (Fig. 5). A mid-day-depression of photosynthetic activities occurred in the 3- and 5-year-old ramets in the Open-patch plots, but was not clearly observed under the other conditions. Models 2-3 and 2-4 were selected for estimating the instantaneous photosynthetic rate in the Beneath- and Edge-patch plots, respectively. Both models did not include *AGE* (Appendix Table 6), and were positively correlated with PPFD. Appendix Table 7 provides details regarding the best generalized linear mixed model for the mid-day-depression rate in Open-patches. Meanwhile, models including *AGE* (i.e., Models 2-1 and 2-2) were selected for the photosynthetic rate in the Open-patch plots for daily measurements. *AGE* negatively affected the photosynthetic rate on all measuring dates. Additionally, *VPD* also negatively influenced the photosynthetic rate, except on October 14, 2013.

Model 4 was used to estimate *DEP* for the ramets in the Open-patch plots, in which mid-day depression was observed. Model 4–1 revealed the logit value of *DEP* increased with *VPD*, and *DEP* increased with the effects of *AGE* (Appendix Table 7). The relationship between *VPD* and *DEP* was simulated in each age class (Fig. 6). The *DEP* value of 0-year-old ramets was less than 0.2, while that of ramets more than 3-year-old was more than 0.8 when the *VPD* value was 2 kPa.

The highest carbon gain per ramet occurred in the Open-patch plots, in which the largest carbon gains were detected in 1-year-old ramets (Fig. 7). We observed a negative carbon gain in the ramets of the Beneath-patch plots after 4 years because the respiration rate was greater than the photosynthetic rate at that time. The carbon gain in the Edge-patch plots was positive through 0–5 years, and largest at 2 years, but was less than 25% of the highest value in the Open-patch plots.

Culm and branch carbon investments were highest in the current-year-old ramets, and rapidly decreased in 1-year-old ramets in every patch. Leaf carbon investment slightly increased in 2-year-old ramets, and gradually decreased in the following years in the Beneath- and Edge-patch plots. Mean while in Open-patch plots, leaf carbon investment started to gradually decrease in 1-year-old ramets.

Although cumulative carbon profit decreased exponentially and had negative values, the mean carbon profit rate increased over time in the Beneath-patch plots (Fig. 8). In the Edge-patch plots, cumulative carbon profit increased from −2 to 6 g $ramet^{-1}$ over 6 years. Additionally, the mean carbon profit rate peaked in 5-year cycles, with slight decreases when the rotation was longer than 5 years. In the Open-patch plot, the cumulative carbon profit peaked in 4-year-old ramets. The carbon profit rate was highest in 2-year cycles, and considerably decreased when the rotation was longer than 2 years. The effect of mid-day-depression on the mean carbon profit rate was small (Fig. 8).

Discussion

The rotation period that provided the most efficient carbon gain almost corresponded to the longevity of the ramets in the Open- (rotation: 2 years; longevity: 1.6–2.2 years) and Edge-patch (rotation: 5 years; longevity: 5.8–8.7 years) plots (Fig. 8). Thus, the hypothesis that the longevity of dwarf bamboo ramets maximizes the efficiency of the carbon budget was partially confirmed by ecophysiological quantification.

The carbon budget model for determining the longevity of a single leaf (Kikuzawa 1991) indicates that longevity is equivalent to the maximum rotation carbon profit rate, which is based on the total carbon gain and cost. Kikuzawa (1991) suggested the carbon profit rate consists of the following three components: (1) initial cost of producing the organ; (2) production rate during the initial stage of growth; (3) decreased production rate

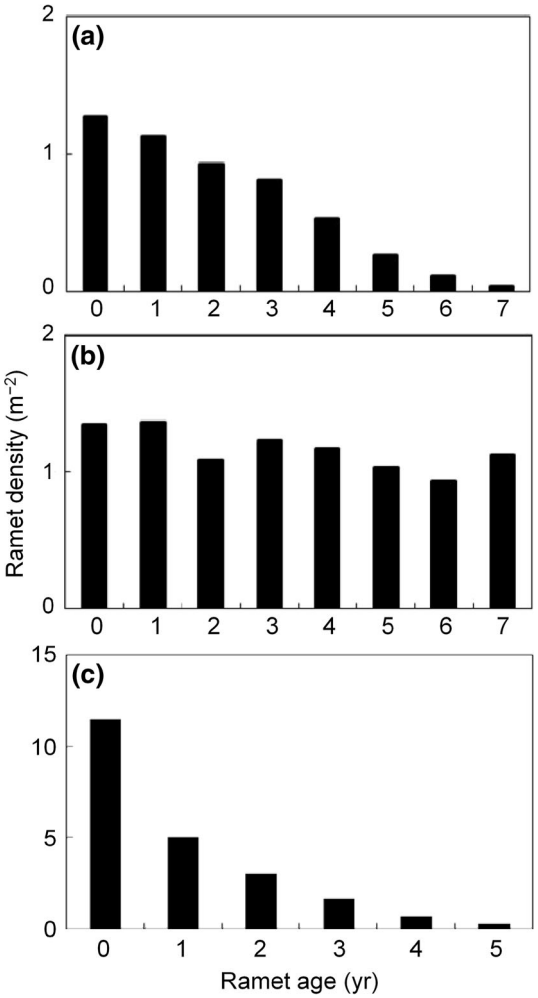

Fig. 2 Ramet density over several years in different patches. Significant differences of mean age were detected between all patches ($P < 0.001$). **a** Beneath-patch, **b** Edge-patch, and **c** Open-patch

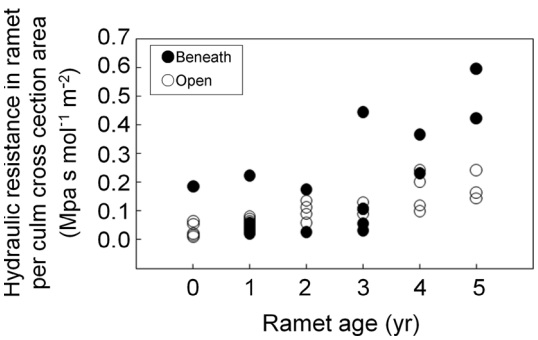

Fig. 3 Relationship between hydraulic resistance and ramet age in Beneath- and Open-patches

during aging. The observed higher initial photosynthetic rate and greater decrease in carbon gain with aging were consistent with the shorter ramet longevity in the Open-patch plots.

This study provided the first evidence that light environment had a significant effect on the longevity of

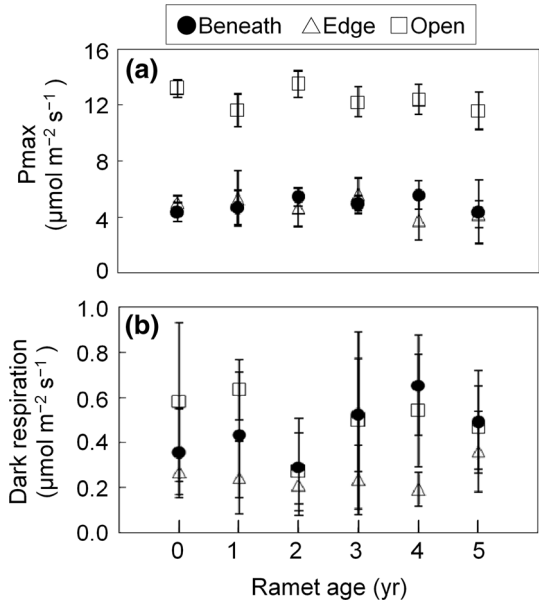

Fig. 4 Relationship between ramet age and **a** maximum gross photosynthetic rate (*Pmax*) and **b** dark respiration rate in current-year leaves. *Error bars* indicate the standard deviation

ramets in *S. kurilensis*. Details regarding *S. kurilensis* ramet longevity was previously limited to the information provided by Yajima et al. (1997), who reported that ramet longevity was 6.3–9.6 years in the understory of a forest. This value range is equivalent to the ramet longevity at the Edge-patch in our study. Our results are partially in accordance with the findings of Kawahara and Tadaki (1978), who reported that the ratio of old culms to the total number of all culms was higher in the understory than in an open area. However, ramet longevity was greatest in the Edge-patch plots under moderate light conditions, and not in the Beneath-patch plots. We address the underlying mechanism regulating the complex light effects on ramet longevity observed in our study in the following section that discusses the within-a-ramet-unit carbon budget. Our findings were inconsistent with the results of a previous study using leaves (Hikosaka 2003).

The annual carbon gain in the Beneath-patch plots was negative in 4- to 7-year-old ramets (Fig. 7, upper panels). This occurred because the culm and branch respiration rates were greater than the net photosynthesis rate in leaves. The cumulative carbon profit decreased with age at a rate that decreased because of reduced carbon investments and not because of changes to the photosynthetic ability per leaf area (Fig. 8). Lei and Koike (1998) revealed that *S. senanensis*, which is a dwarf bamboo species, adapted to environmental conditions beneath the canopy with higher area-based total chlorophyll content, specific leaf area, leaf nitrogen content, and light fleck responses to gain carbon under well-lit conditions during seasons in which phenological gaps occurred (e.g., in early spring and late autumn). We observed that the effects of phenological gaps created

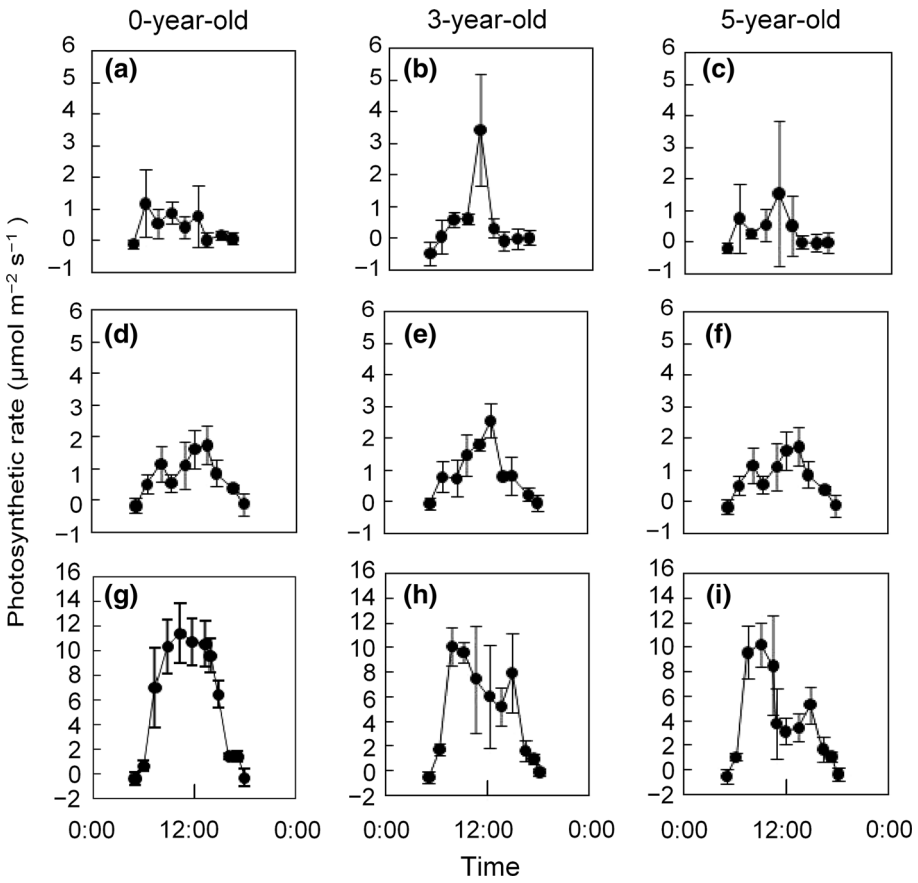

Fig. 5 Diurnal changes in the photosynthetic rate in each patch (*row*) and culm age class (*column*) in September 2012. **a**–**c** Beneath-patch, **d**–**f** Edge-patch, and **g**–**i** Open-patch. *Error bars* indicate the standard deviation

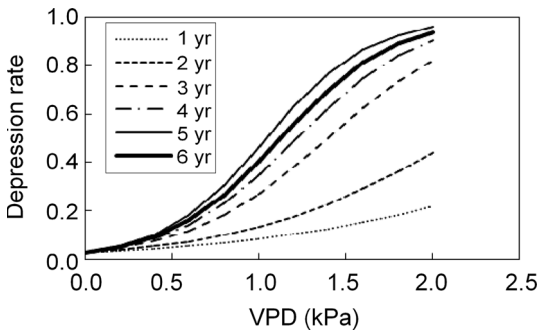

Fig. 6 Estimated mid-day-depression response to vapor pressure deficit (*VPD*) (based on Model 4-1) in open areas (Open-patches)

relatively bright conditions during May and November. However, the ramets lost carbon every year under these conditions. Heavy shading provided less than 2.5% of the relative PPFD in the Beneath-patch plots, which may have prevented a carbon profit each year. Saitoh et al. (2002, 2006) and Saitoh and Seiwa (2007) detected a physiological integration along a light environment gradient from beneath canopies to gaps in *Sasa palmata*. The linkage of ramets between gaps and beneath canopies compensated for decreased carbohydrate production and water and nutrient uptake among ramets. The negative carbon profit in ramets suggests that the carbon resources in the Beneath-patch plots depended on ramets from other patches in a process that Saitoh et al. (2002, 2006) and Saitoh and Seiwa (2007) described as physiological integration.

We assumed the ramets in Beneath-patch plots have two roles. They supply water and nutrients to ramets in well-lit areas and serve as a regeneration bank when new gaps are created. Ramet longevity in the Beneath-patch plots could not be explained by the carbon budget because the ramets in these plots did not contribute to the carbon profit of a genet. The ramets beneath the canopy might supply water and nutrients to ramets in well-lit areas (Saitoh et al. 2002, 2006; Saitoh and Seiwa 2007). They may also serve as a regeneration bank for new gaps, similar to the "seedling bank" of tree species. If the rotation period of a ramet is short, the disadvantages of carbon being consumed for ramet generation may be greater than the advantages resulting from ramet functions. The balance between these functions and carbon consumption for ramet production should be considered when studying ramet longevity. Although the ramet carbon profit was negative and decreased over time, the transition period from positive to negative carbon gain (i.e., 4 years) may be one of the balance points (Fig. 7). However, our results related to the longevity of ramets in the Beneath-patch plots could not be confirmed

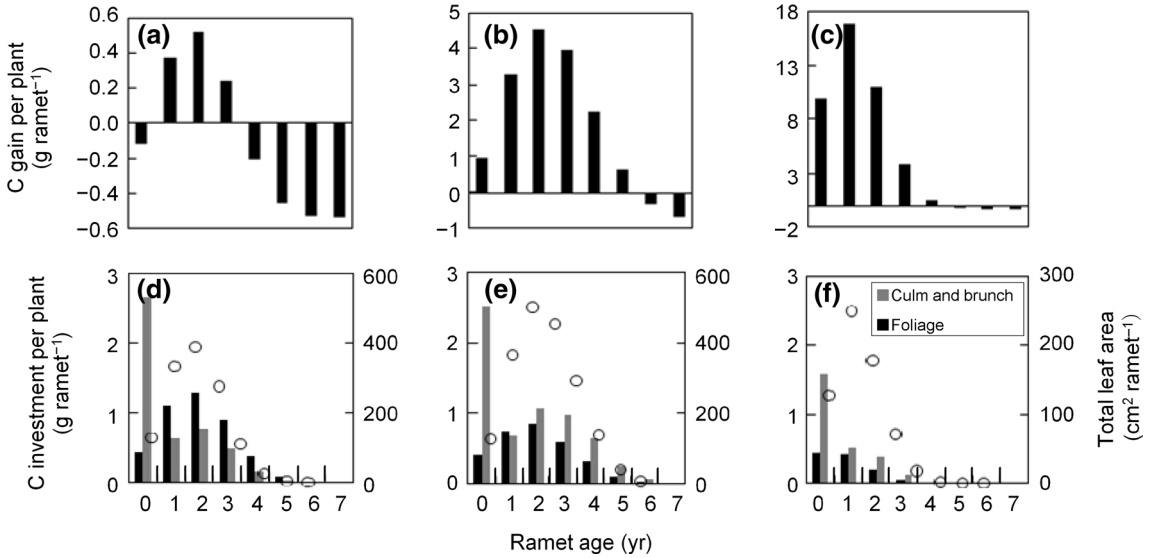

Fig. 7 Carbon budget in each ramet over several years and in different patches. The *upper* and *lower panels* present carbon gain per plant and carbon cost per plant in each patch, respectively. *Open circles* indicate ramet leaf area. **a**, **d** Beneath-patch, **b**, **e** Edge-patch, and **c**, **f** Open-patch

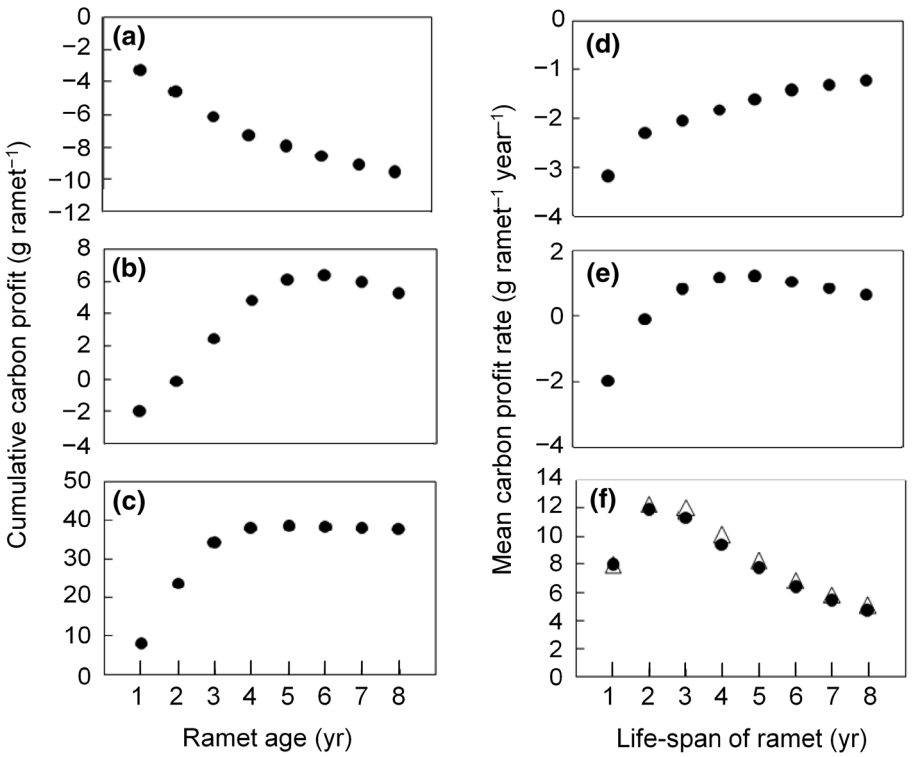

Fig. 8 Relationship between cumulative carbon profit per ramet and ramet age (*left side*) and the relationship between mean annual carbon gain per unit culm weight and ramet lifespan in each patch (*right side*). *Open triangles* indicate the efficiency calculated when mid-day-depression of photosynthetic activity was ignored. **a**, **d** Beneath-patch, **b**, **e** Edge-patch, and **c**, **f** Open-patch

(Fig. 8). Further studies on the function of ramets growing underneath canopies may be useful for clarifying how longevity is determined.

The factor that regulated the considerable decrease in carbon gain in Open-patch ramets was decreasing leaf area due to aging rather than a mid-day-depression of the photosynthetic rate. We assumed that increasing hydraulic resistance with increasing culm age induced a decrease in photosynthetic activity through a mid-day-depression in Open-patches on clear days (Fig. 5; Appendix Table 6). The filling of vessels with impurities, such as tylose in old culms (Kawase et al. 1984), and the

inability to produce new vessels in bamboo tissues are possibly responsible for the observed increase in hydraulic resistance in older culms (Fig. 3; Appendix Table 5). An increase in hydraulic resistance in stems may cause a mid-day-depression (Morikawa and Sato 1976) and lead to a significant drop in productivity, which has been observed even in mesic sites (Tazaki et al. 1980). However, the direct effects of hydraulic resistance on carbon gain through mid-day-depression was assumed to be small. For example, the increasing hydraulic resistance with aging was assumed to raise the depression rate from 5% in current-year-old ramets to 45% in 5-year-old ramets when *VPD* was 1 kPa. However, the increase was from 0.5 to 15% when *VPD* was 0.5 kPa. Because *VPD* exceeded 0.5 and 1.0 kPa for only 42.2 and 16.5% of the entire day, respectively, the total decrease in photosynthetic activities caused by water stress with increasing age was assumed to be small (Fig. 6).

An increase in hydraulic resistance with aging was common in all patches (Fig. 3), but the effects of inhibited water conduction with aging on photosynthesis were negligible in the Beneath- and Edge-patch plots. This was probably due to a shortage of light resources. Light was more of a limiting factor than water stress for photosynthetic rates in the Edge- and Beneath-patch plots. The absence of a mid-day-depression in ramets in the Edge- and Beneath-patch plots (Fig. 5) might have been the reason the leaf photosynthetic rates did not decrease with aging (Appendix Table 7).

The drop in the carbon budget in the Open-patch plots was caused by a rapid decrease in leaf area with aging (Fig. 7, lower panels). This implies carbon investments for creating leaves in older culms decreased over time. One of our hypotheses regarding the reason for the decreases in leaf area with aging involves the reallocation of leaf carbon to the production of new ramets with high water conductivity. In other words, carbon investments to produce new ramets rather than leaves may be more beneficial than investments in old culms. If ramets older than 3-year-old produced the same amount of leaf tissue as 1-year-old ramets, the leaf area of older ramets would be 2.93-times higher than that of current-year ramets. Assuming the water potential is constant, the water flux per leaf area for older ramets would be one-tenth (or lower) of that of current-year-old ramets. This is because hydraulic resistance for the older ramets would be more than 3-times greater than that of current-year-old ramets. This simple estimation suggests that maintaining a constant leaf area in old ramets leads to greater water stress responses, such as a mid-day-depression, than the data produced in this study would indicate. This may lead to the production of new ramets rather than leaves. If the benefit of carbon gain achieved by allocating leaf carbon in new ramets is larger than the carbon cost of producing new ramets, the leaf area will decrease with aging. Thus, increases in hydraulic resistance may indirectly cause a rapid drop in carbon gain in Open-patch plots through a decrease in leaf area, and not directly through a mid-day-depression. The abundance of available water will decrease with age in Edge-patches when a constant leaf area per ramet is assumed. However, the carbon loss caused by decreasing water levels is expected to be small as described above. Additionally, the carbon cost might be relatively high for the production of new ramets with low productivity in Edge-patches, in which this lack of productivity is caused by limited light resources. Thus, the lack of light had a greater effect than the lack of water in Edge-patches, and may have resulted in a moderate decrease in leaf area with aging.

Conclusion

The accuracy of the cost-benefit model in the carbon budget that was used to determine ramet longevity was supported by ecophysiological analyses in the Open- and Edge-patch plots where the carbon gain was positive. The short ramet longevity in the Open-patch plots was due to high initial photosynthetic rates and rapid decreases in leaf area per ramet, but did not directly affect the decrease in photosynthetic activity per leaf area with aging. However, an increase in hydraulic resistance may lead to a rapid loss of leaf area with aging.

Ramet longevity in the Beneath-patch habitat was inconsistent with the rules of the cost-benefit model in the carbon budget because the carbon gain was negative throughout the life span of ramets. This suggests that the carbon investments due to a negative carbon profit and other functions, such as water and nutrient transport to other ramets within a genet, may be determining factors for the longevity of ramets grown in the shade.

Acknowledgements We are grateful to Professors Quan Wang, Masaaki Naramoto, and Atsuhiro Iio for their critical reading of the manuscript, valuable suggestions, and encouragement. We thank Yusuke Kawai for his help in reviewing the literature. We also thank the students of the Silviculture Laboratory, Faculty of Agriculture, Shizuoka University for their helpful comments and support.

Appendix

See Tables 2, 3, 4, 5, 6, 7.

Table 2 Mean monthly temperature during photosynthetic measurements in a preliminary experiment conducted in 2005

Date	Temp (°C)
June 13	14.62
July 19	19.89
August 10	22.70
September 19	17.58
October 14	14.15
November 2	7.38

Table 3 Generalized linear model details for maximum photosynthetic and dark respiration rates with season and leaf age as fixed effects

	Coefficient		
	Estimate	SE	*P*
Pmax			
Intercept (July)	10.84	0.70	< 0.001
Leaf age	−2.38	0.57	< 0.001
June	−0.58	1.14	0.61
August	0.98	0.90	0.28
September	−0.69	0.90	0.44
October	−0.63	0.90	0.49
November	−2.48	0.92	0.0090
Rd			
Intercept (July)	0.42	0.061	< 0.001
Leaf age	−0.20	0.050	< 0.001
June	0.13	0.099	0.18
August	0.19	0.079	0.021
September	0.043	0.079	0.59
October	0.059	0.079	0.45
November	0.040	0.080	0.65

Table 4 Structures of models for estimating hydraulic resistance (*Rh*), instantaneous photosynthetic rate (*Pn*), and mid-day-depression rate (*DEP*)

Response variables Statistic model	R codes for models	
(1) Rh GLM	1-1	Glm (Rh ~ AGE + PATCH, family = gaussian)
	1-2	Glm (Rh ~ AGE, family = gaussian)
	1-3	Glm (Rh ~ PATCH, family = gaussian)
(2) Pn GLM	2-1	Glm (Pn ~ AGE + log (PPFD) + VPD, family = gaussian)
	2-2	Glm (Pn ~ AGE + log (PPFD), family = gaussian)
	2-3	Glm (Pn ~ log (PPFD) + VPD, family = gaussian)
	2-4	Glm (Pn ~ log (PPFD), family = gaussian)
(3) Dep GLMM	3-1	Glmer (Dep ~ AGE: VPD + (1|DATE), family = gaussian (link = "logit"))
	3-2	Glmer (Dep ~ VPD + (1|DATE), family = gaussian (link = "logit"))

GLM generalized linear model, *GLMM* generalized linear mixed model, *AGE* ramet age, *PATCH* measuring patch, *DATE* measuring date, *VPD* vapor pressure deficit

Table 5 Details of the best generalized linear model for hydraulic resistance

Best model: Model 1-1	Coefficient		
	Estimate	SE	*P*
Intercept	1.11×10^{-4}	4.36×10^{-5}	0.021
AGE	4.53×10^{-5}	1.29×10^{-5}	0.003
PATCH-BENEATH	0	–	–
PATH-OPEN	-1.15×10^{-4}	4.34×10^{-5}	0.018

AGE ramet age, *PATCH- BENEATH* Beneath-patch, *PATH-OPEN* Open-patch

Table 6 Details of the best generalized linear models for instantaneous photosynthetic activities on each measuring date

PATCH	DATE	Model type	Variables	Coefficient		
				Estimate	SE	*P*
Beneath	2012/9/7	2-3	Intercept	−1.12	0.11	< 0.001
			VPD	0.65	0.17	< 0.001
			log(PPFD)	0.51	0.035	< 0.001
Edge	2012/9/2	2-4	Intercept	−1.09	0.066	< 0.001
			log(PPFD)	0.56	0.022	< 0.001
Open	2012/9/5	2-1	Intercept	−2.09	0.42	< 0.001
			AGE	−0.34	0.08	< 0.001
			VPD	−0.94	0.41	0.022
			log (PPFD)	1.61	0.09	< 0.001
	2013/8/13	2-1	Intercept	−2.66	0.54	< 0.001
			AGE	−0.63	0.072	< 0.001
			VPD	−2.51	0.65	< 0.001
			log(PPFD)	1.93	0.12	< 0.001
	2013/9/18	2-1	Intercept	−2.61	0.5	< 0.001
			AGE	−0.64	0.07	< 0.001
			VPD	−4.67	0.53	< 0.001
			log(PPFD)	2.29	0.092	< 0.001
	2013/10/14	2-2	Intercept	−3.84	0.39	< 0.001
			AGE	−0.45	0.064	< 0.001
			log(PPFD)	1.88	0.061	< 0.001

AGE ramet age, *PATCH* measuring patch, *DATE* measuring date, *VPD* vapor pressure deficit, *PPFD* photosynthetic photon flux density

Table 7 Details of the best generalized linear mixed model for the mid-day-depression rate in open areas (Open-patches)

Best model 4-1	Coefficient		
	Estimate	SE	*P*
Intercept	−3.51	0.47	< 0.001
AGE-0:VPD	1.23	0.23	< 0.001
AGE-1:VPD	1.64	0.18	< 0.001
AGE-2:VPD	2.52	0.15	< 0.001
AGE-3:VPD	2.88	0.15	< 0.001
AGE-4:VPD	3.36	0.16	< 0.001
AGE-5:VPD	3.12	0.15	< 0.001

AGE ramet age

References

Bassow SL, Bazzaz FA (1998) How environmental conditions affect canopy leaf-level photosynthesis in four deciduous tree species. Ecology 79:2660–2675

Chabot BF, Hicks DJ (1982) The ecology of leaf life spans. Annu Rev Ecol Syst 13:229–259

Hikosaka K (2003) A model of dynamics of leaves and nitrogen in a plant canopy: an integration of canopy photosynthesis, leaf life span, and nitrogen use efficiency. Am Nat 162:149–164

Hikosaka K (2005) Leaf canopy as a dynamic system: ecophysiology and optimality in leaf turnover. Ann Bot 95:521–533

Holbrook NM, Lund CP (1995) Photosynthesis in forest canopies. In: Lowman MD, Nadkami NM (eds) forest canopies. Academic Press, San Diego, pp 411–430

Kawahara T, Tadaki Y (1978) Studies on Sasa communities (III) Relationship between light intensity and biomass of *Sasa nipponica*. J Jpn For Soc 60:244–248 **(in Japanese with English summary)**

Kawase K, Imagawa H, Ujie M (1984) Studies on utilization of *Sasa*-bamboos as forest resources: 1. Physical properties of culms in *Sasa kurilensis*. Res Bull Exp For Hokkaido Univ 41:493–534 **(in Japanese)**

Kikuzawa K (1988) Leaf survivals of tree species in deciduous broad-leaved forests. Plant Species Biol 3:67–76

Kikuzawa K (1989) Ecology and evolution of phenological pattern, leaf longevity and leaf habit. Evol Trend Plants 3:105–110

Kikuzawa K (1991) A cost-benefit analysis of leaf habit and leaf longevity of tree and their geographical pattern. Am Nat 138:1250–1263

Lei TT, Koike T (1998) Functional leaf phenotypes for shaded and open environments of a dominant dwarf bamboo (*Sasa senanensis*) in northern Japan. Int J Plant Sci 159:812–820

Matsumoto Y (1984a) Photosynthetic production in *Abies veitchii* advance growths growing under different light environmental conditions. I. Seasonal growth, crown development, and net production. Bull Tokyo Univ For 73:199–228

Matsumoto Y (1984b) Photosynthetic production in *Abies veitchii* advance growths growing under different light environmental conditions. II. Photosynthesis and respiration. Bull Tokyo Univ For 73:229–252

Morikawa Y, Sato A (1976) Diurnal trends of xylem sap pressure in the crown and sap speed through the trunk in an isolated large *Chamaecyparis obtusa* tree. J Jap For Soc 58:11–14 **(in Japanese with English summary)**

Nakashizuka T (1987) Regeneration dynamics of beech forest in Japan. Vegetatio 69:169–175

Nakashizuka T (1988) Regeneration of beech (*Fagus crenata*) after the simultaneous death of under growing dwarf bamboo (*Sasa kurilensis*). Ecol Res 3:57–67

Nakashizuka T, Numata M (1982) Regeneration process of climax beech forests, I. Structure of a beech forest with the undergrowth of *Sasa*. Jpn J Ecol 32:57–67

Nishimura N, Matsui Y, Ueyama T, Mo W, Saijo Y, Tsuda S, Yamamoto S, Koizumi H (2004) Evaluation of carbon budgets of a forest floor *Sasa senanesis* community in a cool temperate forest ecosystem, central Japan. Jpn J Ecol 54:143–158 **(in Japanese with English summary)**

Oshima Y (1961) Ecological studies of *Sasa* communities. I. Productive structure of some of the *Sasa* communities in Japan. Bot Mag Tokyo 74:199–210

Reich PB, Walters MB, Ellsworth DS (1997) From tropics to tundra: global convergence in plant functioning. Proc Natl Acad Sci USA 94:13730–13734

Reich PB, Ellsworth DS, Walters MB, Vose JM, Gresham C, Volin JC, Bowman WD (1999) Generality of leaf trait relationships: a test acrosssix biomes. Ecology 80:1955–1969

Ryan MG, Yoder BJ (1997) Hydraulic limits to tree height and tree growth. Bioscience 47:235–242

Saitoh T, Seiwa K (2007) Physiological integration of clonal plants: resource acquiring strategies in clonal fragments of a dwarf bamboo, *Sasa palmate*. Jpn J Ecol 57:229–237 **(in Japanese)**

Saitoh T, Seiwa K, Nishiwaki A, Kanno H, Akasaka S (2000) Spatial distribution patterns of *Sasa palmate* in relation to light conditions across gap-understory continuum in beech (*fagus crenata*) forest. J Jpn For Soc 82:342–348 **(in Japanese with English summary)**

Saitoh T, Seiwa K, Nishiwaki A (2002) Importance of physiological integration of dwarf bamboo to persistence in forest understory: a field experiment. J Ecol 90:78–85

Saitoh T, Seiwa K, Nishiwaki A (2006) Effects of resource heterogeneity on nitrogen translocation within clonal fragments of *Sasa palmata*: an isotopic (^{15}N) assessment. Ann Bot 98:657–663

Sakuratani T (1981) A heat balance method for measuring water flux in the stem of intact plants. J Agric Meteorol 37:9–17

Shibata S (1992) Seasonal change of terrestrial parts of three dwarf bamboos. J Jila 55:169–174 **(in Japanese)**

Tazaki T, Ishihara K, Ushijima T (1980) Influence of water stress on the photosynthesis and productivity of plants in humid areas. In: Turner NC, Kramer PJ (eds) Adaptation of plants to water and high temperature stress. Wiley, New York, pp 309–321

Terai Y, Shibata S, Hino T (2009) Effects of herbivorous mammals on aboveground and underground parts of *Sasa nipponica*—the result of the 4th year after the enclosure. J Jpn Soc Reveg Tech 34:516–523

Thornley JHM, Sutcliffe JF, Mahlberg P (1976) Mathematical models in plant physiology. Academic Press, London, pp 92–110

Wijestinghe DK, Hutcings MJ (1997) Heterogeneity on the growth of a clonal plant: an experimental study with *Glechoma hederacea*. J Ecol 85:17–28

Williams K, Field CB, Mooney HA (1989) Relationships among leaf construction cost, leaf longevity, and light environment in rain-forest plants of the genus *Piper*. Am Nat 133:198–211

Wright IJ, Reich PB, Westoby M, Ackerly DD, Baruch Z, Bongers F, Cavendar-Bares J, Chapin T, Cornelissen JHC, Diemer M et al (2004) The leaf economics spectrum worldwide. Nature 428:821–827

Yajima T, Watanabe N, Shibuya M (1997) Changes in biomass of above- and under-ground parts in *Sasa kurilensis* and *Sasa senanensis* stands with culm height. J Jpn For Soc 79:234–238 **(in Japanese with English summary)**